

Analysis of strengthening mechanisms in a severely-plastically-deformed Al–Mg–Si alloy with submicron grain size

D. G. Morris · I. Gutierrez-Urrutia ·
M. A. Muñoz-Morris

Received: 5 May 2006 / Accepted: 13 June 2006 / Published online: 21 December 2006
© Springer Science+Business Media, LLC 2006

Abstract Methods of severe plastic deformation of ductile metals and alloys offer the possibility of processing engineering materials to very high strength with good ductility. After typical amounts of processing strain, a submicrocrystalline material is obtained, with boundaries of rather low misorientation angles and grains containing a high density of dislocations. In the present study, an Al–Mg–Si alloy was severely plastically deformed by equal channel angular pressing (ECAP) to produce such a material. The material was subsequently annealed for dislocation recovery and grain growth. The strength of materials in various deformed and annealed states is examined and the respective contributions of loosely-arranged dislocations, many grain boundaries, as well as dispersed particles are deduced. It is shown that dislocation strengthening is significant in as-deformed, as well as lightly annealed materials, with grain boundary strengthening providing the major contribution thereafter.

Introduction

It is well established that severe plastic deformation processing of ductile metals produces significant hard-

ening, and leaving the materials with respectable ductility for such hardness [1–3]. Typical materials, produced, for example, by equal channel angular pressing of alloys of Al, show a submicron grain microstructure with boundaries of relatively low misorientation angles, and with these fine grains containing a high density of dislocations. While much of the hardening is associated with the fine grain microstructure, a detailed analysis of the role of the grain boundaries, the importance of the significant proportion of low-angle boundaries, and the role of the many retained dislocations has not been made, and is the objective of the present study.

Experimental details

Samples of a commercial 6082 Al alloy (nominally Al-1wt% Mg-1wt% Si, with small amounts of Fe, Mn and Cr present as coarse dispersoids) were heat treated to several different states—solutionization of all Mg and Si at 590 °C and water quenching (state I), subsequent ageing to peak hardening at 250 °C (state II), and overageing at 450 °C (state III)—before severe plastic deformation by equal channel angular pressing (ECAP) at room temperature using a die of angle about 120° producing a strain of 0.7 per pass. Samples were repeatedly deformed, following the so-called route A, to a total strain of 4.2. Subsequently, some of the deformed samples were annealed at temperatures of 200–350 °C to further precipitate any solute remaining in solution, to partially relax the dislocation structure, and to bring about grain growth without recrystallization. Details are found in several publications [4, 5].

D. G. Morris (✉) · I. Gutierrez-Urrutia ·
M. A. Muñoz-Morris
Department of Physical Metallurgy, CENIM, CSIC,
Avenida Gregorio del Amo 8, Madrid 28040, Spain
e-mail: david.morris@cenim.csic.es

Microstructures were examined by scanning and transmission electron microscopy (SEM and TEM), and quantified using standard image analysis methods, to determine grain size and morphology, dislocation density within the grains, as well as size and distribution of fine precipitates and coarser intermetallic dispersoids. Grain boundary misorientations were examined by TEM using converging-beam electron diffraction to obtain Kikuchi line patterns. Mechanical properties were determined by tensile testing with the tensile axis along the long axis of the ECAP-processed cylinders.

Results

Microstructural data of the severely-deformed materials and after further annealing are shown in Table 1 and Fig. 1, and changes of yield stress and tensile ductility in Fig. 2. Further details are given elsewhere [4, 5]. All materials contain 0.5% of stable intermetallic particles of size 100–150 nm with precipitates of β phase (Mg–Si intermetallic) produced during initial annealing (coarse particles) or during annealing after ECAP (fine particles). After ECAP, all materials have submicron elongated grains, with average boundary misorientation of 10–20°, and a high density of dislocations, see Fig. 1(a, b). Annealing at 200 °C leads to fine precipitation, reduction in the dislocation density, and slight grain growth, Fig. 1(c, d) and Table 1. Annealing to 250–300 °C leads to precipitate growth, complete loss of the dislocations, and further grain growth, Table 1.

Tensile testing shows that deformed materials are strong with good ductility. As previously reported, e.g. [1, 2, 4], the maximum load is achieved soon after initial plastic flow, but necking is delayed by a long period of gradual load reduction. Yield stress and ductility values are shown in Fig. 2, for the ECAP-deformed samples and after subsequent annealing. Initially solutionized material (state I) has the best flow stress with good ductility, with subsequent annealing leading to a steady decrease of flow stress and little systematic change of ductility. Some changes of ductility are seen for one material in the as-deformed state, and for another material after high-temperature annealing, effects due to precipitate dissolution and partial recrystallization [4].

Discussion

The present discussion will concentrate on the evaluation of the strengthening contributions of each of the microstructural features—fine grain size, boundaries with a range of misorientations, fine and coarse particles, high dislocation density. Other aspects, such as the role of solute, fine precipitate particles and coarse dispersoid particles on deformation microstructure and stability on annealing have been discussed elsewhere [4, 5], and will not be examined here.

The most important analysis of strengthening contributions is presented in Fig. 3, showing a Hall-Petch analysis of the measured flow stresses for materials in the various as-ECAP conditions and after subsequent annealing.

Table 1 Particle volume fractions and sizes, yield stress and Orowan stress contribution, and grain sizes in ECAP-deformed and subsequently heat treated materials

Material: Annealed state	Volume of particles (%)			Average particle size (nm)			Yield stress (MPa)	Orowan stress (MPa)	Grain size (μm). (Fraction recrystallized)
	IM	β_C	β_P	IM	β_C	β_P			
I (ECAP)	0.5	–	–	135	–	–	330	14	0.25
I + 200 °C	0.5	–	1.5	135	–	85	256	53	0.32
I + 250 °C	0.5	–	1.5	135	–	100	211	48	0.40
I + 300 °C	0.5	–	1.5	135	–	100	183	48	0.7 (25% – 2.0)
II (ECAP)	0.5	–	–	135	–	–	316	14	0.3
II + 200 °C	0.5	–	1.5	135	–	80	233	54	0.37
II + 250 °C	0.5	–	1.5	135	–	95	208	49	0.40
II + 300 °C	0.5	–	1.5	135	–	110	171	45	0.63
III (ECAP)	0.5	0.9	–	135	500	–	309	20	0.35
III + 200 °C	0.5	0.9	0.5	135	610	70	227	44	0.46
III + 250 °C	0.5	0.9	0.5	135	680	75	178	41	0.43 (25% – 0.74)
III + 300 °C	0.5	0.9	0.5	135	800	85	134	38	0.74 (50% – 3.2)

Particles are stable intermetallics (IM), fine precipitates (β_P) and coarse particles (β_C). Grain size is given also for some recrystallized fraction after high temperature annealing

Fig. 1 Transmission electron micrographs (bright field and weak beam) showing grain and dislocation structures in material II: (a–b) as ECAP-deformed; (c–d) annealed for 1 h at 200 °C. Weak beam images taken in a $g: 4g$ condition, with a 111 g vector

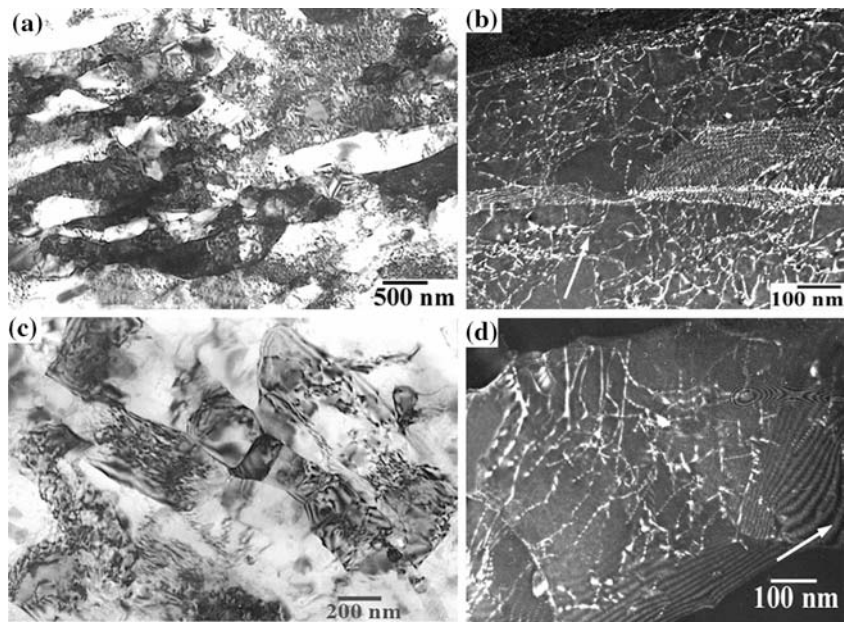


Fig. 2 Effect of annealing treatments on yield stress and ductility of materials initially processed to states I, II and III, deformed by ECAP to a strain of 4.2, and then annealed for 1 h at temperature

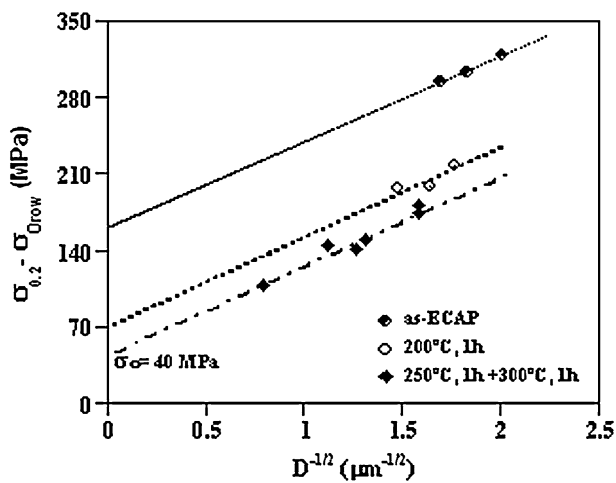
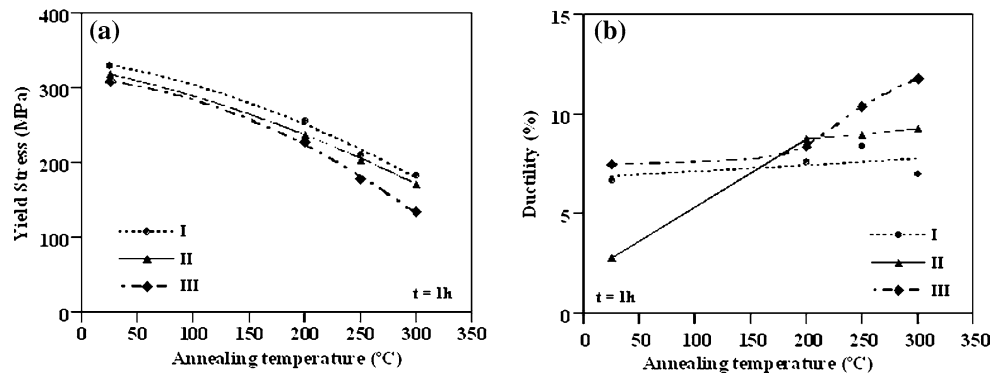


Fig. 3 Hall-Petch analysis relating the experimental flow stress, after removal of a particle strengthening contribution, of materials I, II and III in the as-ECAP deformed state and after annealing at 200, 250 and 300 °C

All the present materials will be strengthened by several contributions: (i) that due to fine grain size, with boundaries ranging from very high angle to very low angle varieties; (ii) that due to the dislocations present within the materials, many in the as-deformed state and few after annealing at high temperatures; (iii) that due to coarse dispersoid particles and fine or coarse precipitates; and (iv) that due to the matrix with some quantity of Mg and Si in solution.

A first stage of analysis involves the removal of the strengthening contribution due to precipitate and dispersoid particles. In all cases the particles present are relatively large, and their size and size distribution has been determined from many SEM and TEM photographs. It is assumed that the contribution of each particle species is that calculated from the Orowan model, and can be added linearly to the other strengthening contributions (grain size, matrix, dislocations). This assumption of linear addition has been

justified when relatively few, strong obstacles are present together with many weaker obstacles [5, 6].

Following removal of the Orowan particle strengthening contribution, we attempt to separate grain boundary and other strengthening contributions using a Hall-Petch analysis, as shown in Fig. 3. Here, the good linear dependence of strength with reciprocal square root of grain size for each state of annealing is taken as confirmation of the validity of this Hall-Petch analysis. We can separate the materials examined into three categories: as-deformed, with the very high dislocation density; after slight annealing at 200 °C, with a moderate dislocation density; and after high-temperature annealing, with essentially no dislocations within the grains. For each category of material the Hall-Petch slope is the same, 78 MPa $\sqrt{\mu\text{m}}$, and the intercept stress (σ_0) falls with annealing from 160 MPa to 70 MPa and 40 MPa.

Several aspects of this analysis are worthy of discussion. Firstly, we have considered above that all boundaries should be used in the Hall-Petch analysis, irrespective of the misorientation at the boundary. As mentioned earlier, the average boundary misorientation was 10–20°, and we can consider about one third of the boundaries present to be low angle grain (or subgrain) boundaries (LAGB), with about another third being medium angle grain boundaries (MAGB) and another third being high angle grain boundaries (HAGB). It is worth considering whether LAGB should be included in the Hall-Petch analysis. Firstly, we may note that the experimental Hall-Petch slope will change to about 110 MPa $\sqrt{\mu\text{m}}$ if we exclude the third of LAGB from our analysis, which seems rather high for an only slightly alloyed Al–Mg–Si matrix [5, 7], while the value deduced considering all boundaries, 78 MPa $\sqrt{\mu\text{m}}$, seems very reasonable.

A second way of looking at this analysis is to examine the question of when a boundary is likely to be strong enough to be an effective barrier to an incoming dislocation and to act as a (Frank-Read) source for new dislocation generation in the downstream grain. As reported recently by Hansen [8], the Hall-Petch slope k may be written as:

$$k = M \sqrt{\frac{\tau^{\text{GB}} \cdot Gb}{\pi k_\gamma}} \quad (\text{i})$$

where M is the Taylor factor, τ^{GB} is the stress concentration at the grain boundary, where the Frank-Read source of new dislocations is operating, G and b are the shear modulus and the Burgers vector, respectively, and k_γ is a constant between 1 and $1-\nu$, the Poisson's ratio. Substituting in reasonable values

for all these parameters, and considering that the Frank-Read source width is about 10^{-8} to 10^{-7} m (i.e. equivalent to a dislocation density of 10^{14} – 10^{16} m^{-2} , the same as that measured within the grains of as-deformed materials, 10^{15} m^{-2}) we deduce a Frank-Read source strength (τ^{GB}) of about 75–750 MPa and a theoretical Hall-Petch slope of 45–140 MPa $\sqrt{\mu\text{m}}$, well consistent with the experimental value. At a LAGB, considered as a dislocation cell wall, incoming dislocations may manage to squeeze through gaps in the cell walls in a similar manner to the operation of a Frank-Read source. The strength of such gaps is estimated, considering that the dislocation spacing defines a Frank-Read source length, as:

$$\tau_{\text{FR}} = G\theta / \pi \quad (\text{ii})$$

where θ is the misorientation at the LAGB. How large a misorientation is required for the boundary to be as strong as a general grain boundary? Equation (ii) shows a boundary strength of about 140 MPa per degree of misorientation. Hence those LAGB with misorientations of a few degrees can already be considered as strong obstacles. In this case, the Hall-Petch slope can be estimated as:

$$k = M\alpha G\sqrt{(3b\theta)} \quad (\text{iii})$$

where α is a constant of value about 0.25. According to this equation, a LAGB very quickly becomes as strong a Hall-Petch strengthener as a general grain boundary. The boundary strength could be considerably reduced, however, if an incoming dislocation is considered able to cut through the boundary dislocations, one by one, and such very low angle boundaries may then not be sufficiently strong.

From the arguments presented above, it is obvious that all boundaries apart from those of extremely low misorientations (e.g. $<5^\circ$) can be considered as strong strengtheners, and the Hall-Petch analysis of Fig. 3, taking account of essentially all the boundaries present, is reasonably justified.

A second aspect of the Hall-Petch analysis of Fig. 3 worthy of consideration is that we deduce a similar slope for as-deformed materials, with essentially all the 1%Mg-1%Si in solution, and for materials annealed at 200–250–300 °C, where much of these elements will be out of solution in the form of precipitates. This point is interesting since, for the case of alloys with bcc matrix, a strong solution effect on hardening has been noted Nieh, T.G., pers. comm. In the present case, the solute content changes from approximately 2% for solutionized and as-deformed materials (i.e. states I and II)

(since the ECAP deformation is determined to essentially completely redissolve any fine precipitates present [4, 5]) to approximately 0.5% for those materials annealed at low temperatures after ECAP. This change of solute content is perhaps too small to produce any significant change in material mechanical behaviour, or otherwise the fcc alloys are indeed different from bcc alloys in showing a very weak solution effect on strengthening.

As a final point we may examine the values of the stress intercept σ_0 in Fig. 3, namely 160–70–40 MPa for as-deformed, 200 °C-annealed and 250/300 °C-annealed materials. The 40 MPa value corresponds well with that expected for a dilute Al solution (only about ½% of Mg + Si in solution) with no grain boundary or dislocation strengthening contributions. The important difference between as-deformed and annealed materials is the high dislocation density retained within the grains, see Fig. 1. The difference of stress intercepts $\Delta\sigma$ (120 MPa and 30 MPa) can be interpreted as:

$$\Delta\sigma = M \alpha bG\sqrt{\rho} \quad (\text{iv})$$

where ρ is the dislocation density inside the grains. Values of about $5 \times 10^{14}/\text{m}^2$ and $3 \times 10^{13}/\text{m}^2$ are deduced to be necessary to produce this strengthening. Both values are in excellent agreement with measurements of dislocation densities made from micrographs such as those of Fig. 3(b and d), namely about $10^{15}/\text{m}^2$ and $10^{14}/\text{m}^2$, respectively.

Conclusions

The strength of severely-deformed Al alloy has been examined and the relative contributions of grain boundaries of varying degrees of misorientation, of

dislocations found within those grains, and of precipitate/dispersoid particles within these materials has been evaluated. For the particular materials examined, it is shown that the strengthening contribution of each term is approximately equal for as-deformed materials, with dislocation hardening and grain boundary hardening contributing equal amounts. It is shown that boundaries become sufficiently strong to contribute significantly to hardening once their misorientation exceeds a few degrees only. On annealing the present materials, the dislocations quickly annihilate while grain growth is slow: strength evolution is explained by the variation of the contributions of these microstructural features.

Acknowledgements We would like to thank the Comunidad de Madrid for financial support for part of this work under contract no. 07N/0087/2002.

References

1. Furukawa M, Horita Z, Nemoto M, Valiev RZ, Langdon TG (1998) *Phil Mag* 78A:203
2. Hayes JS, Keyte R, Prangnell PB (2000) *Mater Sci Technol* 16:1259
3. Valiev RZ, Alexandrov IV, Zhu YT, Lowe TC (2002) *J Mater Res* 17:5
4. Gutierrez-Urrutia I, Muñoz-Morris MA, Morris DG (2005) *Mater Sci Eng* 394A:399
5. Gutierrez-Urrutia I, Muñoz-Morris MA, Morris DG (2006) *J Mater Res* (in press)
6. Brown LM, Ham RK (1971) In: Kelly A, Nicholson RD (eds) *Strengthening methods in crystals*, Elsevier, Amsterdam, The Netherlands
7. Armstrong RW, Douthwaite RM (1995) In: Otonari MA, Armstrong RW, Grant NJ, Ishizaki K (eds) *Grain size and mechanical properties—Fundamentals and applications*, Mater. Res. Soc. Symp. Proc. 362, Pittsburgh, PA, p 41
8. Hansen N (2005) *Adv Eng Mater* 7:815